6240 *Inorg. Chem.* **2010**, *49*, 6240–6252
DOI: 10.1021/ic100261b

Inorganic Chemistry
Forum Article

Electronic Structure and Dynamics of Nitrosyl Porphyrins

W. Robert Scheidt,*,† Alexander Barabanschikov,‡ Jeffrey W. Pavlik,† Nathan J. Silvernail,† and J. Timothy Sage*,‡

†*Department of Chemistry and Biochemistry, University of Notre Dame, Notre Dame, Indiana 46556, and* ‡*Department of Physics and Center for Interdisciplinary Research on Complex Systems, Northeastern University, Boston, Massachusetts 02115*

Received February 8, 2010

Nitric oxide (NO) is a signaling molecule employed to regulate essential physiological processes. Thus, there is great interest in understanding the interaction of NO with heme, which is found at the active site of many proteins that recognize NO, as well as those involved in its creation and elimination. We summarize what we have learned from investigations of the structure, vibrational properties, and conformational dynamics of NO complexes with ferrous porphyrins, as well as computational investigations in support of these experimental studies. Multitemperature crystallographic data reveal variations in the orientational disorder of the nitrosyl ligand. In some cases, equilibria among NO orientations can be analyzed using the van't Hoff relationship and the free energy and enthalpy of the solid-state transitions evaluated experimentally. Density functional theory (DFT) calculations predict that intrinsic barriers to torsional rotation are smaller than thermal energies at physiological temperatures, and the coincidence of observed NO orientations with minima in molecular mechanics potentials indicates that nonbonded interactions with other chemical groups control the conformational freedom of the bound NO. In favorable cases, reduced disorder at low temperatures exposes subtle structural features including off-axis tilting of the Fe−NO bond and anisotropy of the equatorial Fe−N bonds. We also present the results of nuclear resonance vibrational spectroscopy measurements on oriented single crystals of [Fe(TPP)(NO)] and [Fe(TPP)(1-MeIm)(NO)]. These describe the anisotropic vibrational motion of iron in five- and six-coordinate heme−NO complexes and reveal vibrations of all Fe−ligand bonds as well as low-frequency molecular distortions associated with the doming of the heme upon ligand binding. A quantitative comparison with predicted frequencies, amplitudes, and directions facilitates identification of the vibrational modes but also suggests that commonly used DFT functionals are not fully successful at capturing the trans interaction between the axial NO and imidazole ligands. This supports previous conclusions that heme−NO complexes exhibit an unusual degree of variability with respect to the computational method, and we speculate that this variability hints at a genuine electronic instability that a protein can exploit to tune its reactivity. We anticipate that ongoing characterization of heme−NO complexes will deepen our understanding of their structure, dynamics, and reactivity.

Introduction: Recognition of Diatomic Molecules

Molecular recognition is the foundation of biological regulation. Typically, variations in shape and charge distribution distinguish biological macromolecules (proteins and nucleic acids).[1,2] Biomolecular recognition often relies on their characteristic structural flexibility as well.[3] In addition to macromolecular messengers such as hormones or antibodies, the smallest biomolecules[4] also play essential roles in biological signaling.

Diatomic molecules possess physical properties, such as facile diffusion and high membrane permeability, that make them uniquely useful as rapid-response cellular and intracellular messengers. On the other hand, the three best established members of the human "diatome" seem barely distinguishable on the basis of size, shape, and polarity (Table 1). At first glance, the specific recognition of nitric oxide (NO) by soluble guanylate cyclase in the presence of cellular dioxygen (O_2) concentrations typically 3 orders of magnitude higher[5,6] appears to be a tall order. The enormous variation in the magnetic moment is intriguing, but it is not immediately apparent how these differences can be exploited.

*To whom correspondence should be addressed. E-mail: Scheidt.1@nd.edu (W.R.S.), jtsage@neu.edu (J.T.S.). Fax: (574) 631-6652 (W.R.S.), (617) 373-2943 (J.T.S.).

(1) Janin, J.; Bahadur, R.; Chakrabarti, P. *Q. Rev. Biophys.* **2008**, *41*, 133–180.
(2) Rohs, R.; West, S.; Liu, P.; Honig, B. *Curr. Opin. Struct. Biol.* **2009**, *19*, 171–177.
(3) Smock, R.; Gierasch, L. *Science* **2009**, *324*, 198–203.
(4) Ghosh, A., Ed. *The Smallest Biomolecules: Diatomics and their Interactions with Heme Proteins*; Elsevier BV: Amsterdam, The Netherlands, 2008.
(5) Cary, S. P. L.; Winger, J. A.; Derbyshire, E. R.; Marletta, M. A. *Trends Biochem. Sci.* **2006**, *31*, 231–239.
(6) Hall, C.; Garthwaite, J. *Nitric Oxide* **2009**, *21*, 92–103.

 Published on Web 07/12/2010

Table 1. Selected Physical Properties of Diatomic Molecules (from the Computational Chemistry Comparison and Benchmark Database, NIST Standard Reference Database Number 101, Release 14, Sept 2006, Johnson, R. D., III, Ed., http://srdata.nist.gov/cccbdb)

	bond length (pm)	dipole moment/*e* (pm)	spin
CO	112.83	2.3	0
NO	115.08	3.1	$^1/_2$
O_2	120.75	0.0	1

Biology exploits many useful properties of hemes, including the availability of multiple oxidation states of iron and their ability to bind small ligands. Heme complexes with diatomic ligands exhibit characteristic variations in the structure and charge distribution that nature exploits to solve the signaling conundrum described above. Discrimination between heme derivatives of carbon monoxide (CO) and O_2 is relatively well understood. In particular, electron transfer from ferrous iron to the bound O_2 upon binding to heme[7] facilitates hydrogen-bond donation to the bound O_2.[9−12] The energetic cost of molecular adjustments to accommodate the differing equilibrium geometries of the heme−CO and heme−O_2 complexes, while potentially significant as well,[8] are smaller in magnitude than the energetic stabilization of the heme−O_2 complex by hydrogen bonding in the globins.[9−13]

The electronic structure of heme−NO complexes is also of great interest because of their contribution to biological signaling processes and is more variable because of a tendency to lose the axial ligand trans to NO. However, the predicted electronic structure depends significantly on the computational method used. Comparison with quantitative experimental input will be essential to directly characterize the structure, dynamics, and reactivity of heme−NO complexes.

In this *Inorganic Chemistry* Forum, we develop what we have learned about NO behavior and NO dynamics from a variety of approaches that includes experimental structure determinations, vibrational spectroscopy measurements, and theoretical calculations in support of these experimental results.

Structural Aspects

Solid-State Structures. Early X-ray structure determinations of nitrosyl iron porphyrinate derivatives showed that the NO ligand often samples multiple conformations. This phenomenon is applicable to the iron species with distinctly nonlinear FeNO groups; Fe−N−O bond angles are found in the range of 140−150°. These are considered {FeNO}^{7} species in the Enemark and Feltham notation[14] and can be nominally considered to be iron(II)

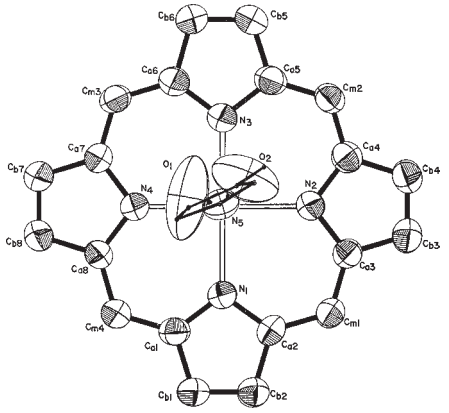

Figure 1. ORTEP diagram (50% probability ellipsoids) of the core of [Fe(TPP)(1-MeIm)(NO)] and the axial ligands. The atoms of the imidazole ligand trans to the NO have been drawn arbitrarily small. Note the large thermal motion of the oxygen atom corresponding to the two orientations of the NO ligand compared to the other atoms in the structure. The phenyl groups are omitted. Reproduced from ref 16.

derivatives. Alternatively, or in addition to site disorder, the nitrogen and oxygen atoms display anomalously large thermal motion consistent with extensive spatial excursions of the nitrogen or oxygen atom. Both phenomena are indicative of a rather facile rotation of the NO ligand around the Fe−N(NO) bond. Early examples of multiple-site systems included the five-coordinate complex [Fe(TPP)(NO)],[15] which displayed eight distinct sites for the NO ligand in the solid-state structure (four on each side of the porphyrin plane), and six-coordinate [Fe(TPP)(1-MeIm)(NO)],[16] which displayed substantial thermal motion for the NO ligand atoms and a minimum of two distinct NO sites, as displayed in Figure 1. The difference in thermal motion between the terminal oxygen atoms and other atoms of the molecule elicited concerns by one of the reviewers of the original paper![17] However, all subsequent analyses of this complex are consistent with the measurement being fundamentally right. Another early six-coordinate system, [Fe(TPP)(4-MePip)(NO)],[18] has two polymorphs; both have an apparent single orientation of NO but again with large thermal motion for the terminal oxygen atom.

Recent developments from the solid-state structure determinations of nitrosyl porphyrinate derivatives have provided new insight into the dynamics of NO motion in the solid state. The majority of these new structural studies were carried out as a prelude to nuclear resonance vibrational spectroscopy (NRVS) studies utilizing oriented single-crystal samples. The redetermination of the structure of [Fe(TPP)(1-MeIm)(NO)][19] at 100 K showed

(7) Chen, H.; Ikeda-Saito, M.; Shaik, S. *J. Am. Chem. Soc.* **2008**, *130*, 14778–14790.
(8) Sage, J. T. Hemoglobins: O_2 Uptake and Transport. In *Encyclopedia of Supramolecular Chemistry*; Atwood, J., Steed, J. W., Eds.; Marcel Dekker: New York, 2004.
(9) Springer, B. A.; Sligar, S. G.; Olson, J. S.; Phillips, G. N., Jr. *Chem. Rev.* **1994**, *94*, 699–714.
(10) Spiro, T. G.; Kozlowski, P. M. *Acc. Chem. Res.* **2001**, *34*, 137–144.
(11) Sigfridsson, E.; Ryde, U. *J. Inorg. Biochem.* **2002**, *91*, 101–115.
(12) Birukou, I.; Schweers, R. L.; Olson, J. S. *J. Biol. Chem.* **2010**, *285*, 8840−8854.
(13) The following abbreviations are used in this paper: NO, nitric oxide; Porph, generalized porphyrin dianion; TPP, dianion of *meso*-tetraphenylporphyrin; OEP, dianion of octaethylporphyrin; T*p*FPP, dianion of *meso*-*p*-fluorotetraphenylporphyrin; T*p*OCH$_3$PP, *meso*-*p*-methoxytetraphenylporphyrin; 1-MeIm, 1-methylimidazole; 4-MePip, 4-methylpiperidine NRVS, nuclear resonance vibrational spectroscopy; VDOS, vibrational density of states.
(14) Enemark, J. H.; Feltham, R. D. *Coord. Chem. Rev.* **1974**, *13*, 339–406.
(15) Scheidt, W. R.; Frisse, M. E. *J. Am. Chem. Soc.* **1975**, *97*, 17–21.
(16) Scheidt, W. R.; Piciulo, P. L. *J. Am. Chem. Soc.* **1976**, *98*, 1913–1919.
(17) Although one of the two reviewers was quite laudatory, a second was quite critical of the experimental results and the conclusions. Comments included "The authors ... did produce some figures which are indicative of excessive motion of O_1 and O_2. [The NO oxygen atoms] Such motion and disorder..." and continued with strongly negative comments concerning the idea that NO is a good trans-labilizing ligand. After some revision and extensive discussions with the Associate Editor, the paper was accepted for publication.
(18) Scheidt, W. R.; Brinegar, A. C.; Ferro, E. B.; Kirner, J. F. *J. Am. Chem. Soc.* **1977**, *99*, 7315–7322.
(19) Wyllie, G. R. A.; Schulz, C. E.; Scheidt, W. R. *Inorg. Chem.* **2003**, *42*, 5722–5374.

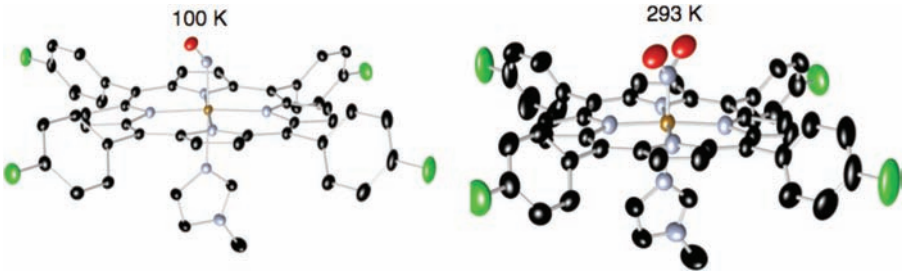

Figure 2. ORTEP diagrams (50% probabiliity ellipsoids) of the triclinic polymorph of [Fe(T*p*FPP)(1-MeIm)(NO)] at 100 and 293 K. No experimental evidence for a second orientation of NO at 100 K is evident in the difference Fourier maps. Reproduced from ref 21.

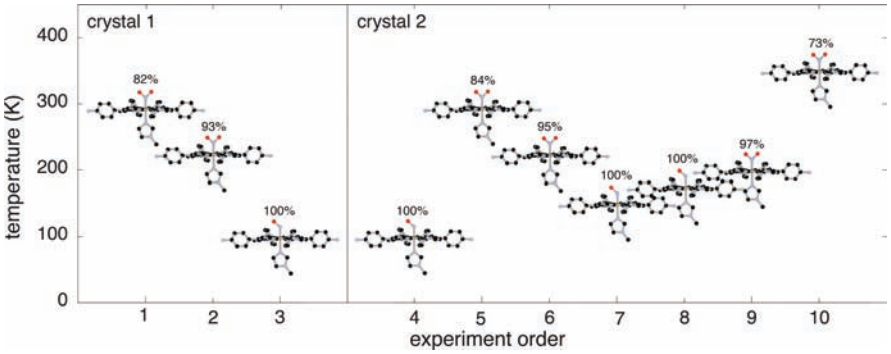

Figure 3. Diagram illustrating the order of data acquisition for the triclinic polymorph of [Fe(T*p*FPP)(1-MeIm)(NO)]. The temperature of data acquisition and the occupancy factors for the major orientations are also displayed. Reproduced from ref 21.

that the NO ligand disorder was still present, but with distinctly different orientations of the NO ligand compared to the original (room temperature) structure. A subsequent room temperature redetermination of [Fe(TPP)(1-MeIm)(NO)] with higher resolution data than the original determination revealed that the NO disorder was more likely that of three distinct NO sites.[20] These observations are clearly consistent with the idea of facile rotation of the NO ligand around the Fe−N(NO) bond. Silvernail et al.[21] then observed that three different six-coordinate nitrosyl derivatives, [Fe(Porph)(1-MeIm)(NO)] where Porph = T*p*FPP (two forms) or T*p*OCH$_3$PP, showed temperature-dependent populations of nitrosyl sites. In the solid state, each of these systems displayed a *single* NO orientation at low temperature, but at varying higher temperatures (above 150 K), all three derivatives developed a second orientation of NO. Interestingly, the amounts of NO rotation about the Fe−N(NO) bond in the three derivatives were distinctly different. The structures for the triclinic polymorph of [Fe(T*p*FPP)(1-MeIm)(NO)] at 100 and 293 K are given in Figure 2. Each of these three derivatives displayed distinctly different relative orientations of the coordinated NO. The magnitude of the population of the second site, as defined by X-ray analysis, was not only temperature-dependent but also sensibly temperature-dependent. This can be seen from Figure 3, which displays the temperature chronology of structure determinations from two different crystalline samples. X-ray diffraction experiments with varying temperature (in both increasing and decreasing temperature regimes) and different crystal specimens showed that the order/disorder phenomenon was reproducible and reversible. These observations are consistent with control of the NO orientation by crystal packing effects. Decreasing the temperature of the crystalline solid leads to smaller unit cells and molecular volumes that yield slightly tighter intermolecular contacts that lead to a single site for the NO group. Interestingly, none of the nitrosyl systems examined displays an unusually large contraction of the unit cell upon cooling. A more detailed analysis of the temperature-dependent effects of the intermolecular contacts and the ramifications is given in the next section.

In a related five-coordinate system, the extensive 8-fold disorder in [Fe(TPP)(NO)] [4-fold NO rotations around the Fe−N(NO) bond on each side of the porphyrin plane][15] coalesces to a single NO site on each side of the porphyrin plane as the temperature is lowered.[22] This ordering of the NO site is the result of a crystallographic phase change from a high-symmetry tetragonal crystal system to the much lower symmetry triclinic crystal system. The only molecular symmetry element retained in the phase transition is an inversion center at the center of the porphyrin ring. Diffraction experiments pointed to a phase change transition over a rather gradual temperature range centered at ~250 K. The phase change is temperature-dependent and reversible based on the diffraction results on several independent crystal preparations. Indeed, one crystal was cooled and the structure determined at a temperature as low as 33 K without any apparent effect on either the crystallinity or the reversibility of the phase change. The reason for the phase

(20) Silvernail, N. J.; Barabanschikov, A.; Sage, J. T.; Noll, B. C.; Scheidt, W. R. *J. Am. Chem. Soc.* **2009**, *131*, 2131–2140.
(21) Silvernail, N. J.; Pavlik, J. W.; Noll, B. C.; Schulz, C. E.; Scheidt, W. R. *Inorg. Chem.* **2008**, *47*, 912–920.
(22) Silvernail, N. J.; Olmstead, M. M.; Noll, B. C; Scheidt, W. R. *Inorg. Chem.* **2009**, *48*, 971–977.

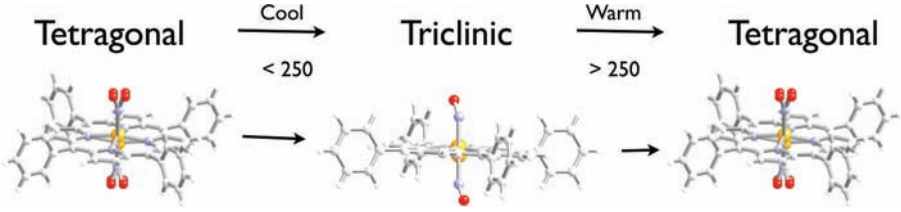

Figure 4. Diagram illustrating the changes in the solid-state structure of [Fe(TPP)(NO)] as the crystalline sample is warmed and cooled. Reproduced from ref 22.

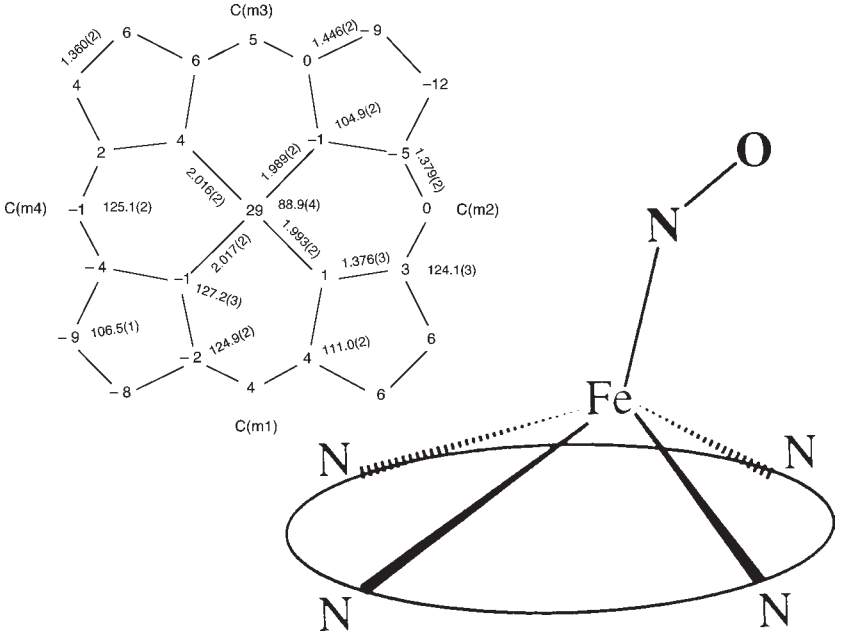

Figure 5. Diagram illustrating the axial tilt observed in [Fe(OEP)(NO)] and its effect on the equatorial bond distances. The NO tilts toward C(m2), and those equatorial distances are seen to be shorter than those opposite the NO tilt. This pattern has been seen in all cases where it is possible to observe. Reproduced from refs 21 and 24.

change and the resultant ordering of the disordered NO are not completely clear. The relatively small changes in the temperature-dependent cell volumes of [Fe(TPP)(NO)] suggest that differences in packing efficiencies are not a major driving force for the phase change (Figure 4). What then does lead to the NO ordering and the phase change?

We had previously suggested[22] that an unusual structural feature of coordinated nitrosyl in the {FeNO}^{7} systems, observed originally in two crystalline forms of [Fe(OEP)(NO)][23] and subsequently in other five-coordinate nitrosyl derivatives,[24] could be the driving force for a molecular structural change and, hence, a phase change. Several ordered five-coordinate derivatives[23−25] were found to all display an off-axis tilting of the Fe−N(NO) bond. In addition, this axial tilting was observed to be correlated with a small but statistically significant asymmetry in the equatorial Fe−N_p bonds. A diagram illustrating the off-axis tilting and core asymmetry is given in Figure 5. In this view, the molecular asymmetry is increasingly favored at lower temperature, and when molecular distortion occurs, the entire lattice makes small adjustments in the intermolecular packing that lead to the descent to the lower symmetry space group and a single Fe−NO orientation on each side of the porphyrin plane. Support for this view came from the observation that the lower symmetry unit cell had four differing crystal domains with relative rotations of 90 or 180° with respect to the major domain, with the rotations occurring along the original (tetragonal) Fe−N(NO) direction. This is consistent with the NO tilt "catalyzing" the transition.

[Co(TPP)(NO)] shows the same 8-fold disorder[26] at room temperature as the analogous iron derivative; the off-axis tilting of the Co−N(NO) bond and core asymmetry are also observed in an ordered form of [Co(OEP)(NO)].[27] We thus expected that similar temperature-dependent order/disorder phenomena would be seen in [Co(TPP)(NO)]. Indeed, the NO ordering was observed along with some informative differences between the cobalt and iron systems.[28] The transition from the tetragonal crystal system to the triclinic phase occurs over a much smaller temperature range centered around 195 K. In addition, an apparent transition structure was observed near the transition temperature. As shown in Figure 6,

(23) Ellison, M. K.; Scheidt, W. R. *J. Am. Chem. Soc.* **1997**, *119*, 7404–7405.
(24) Scheidt, W. R.; Duval, H. F.; Neal, T. J.; Ellison, M. K. *J. Am. Chem. Soc.* **2000**, *122*, 4651–4659.
(25) Bohle, D. S.; Debrunner, P.; Fitzgerald, J.; Hansert, B.; Hung, C.-H.; Thompson, A. J. *J. Chem. Soc., Chem. Commun.* **1997**, 91–92.
(26) Scheidt, W. R.; Hoard, J. L. *J. Am. Chem. Soc.* **1973**, *95*, 8281–8288.
(27) Ellison, M. K.; Scheidt, W. R. *Inorg. Chem.* **1998**, *37*, 382–383.
(28) Grande, L. M.; Noll, B. C.; Oliver, A. G.; Scheidt, W. R., manuscript submitted.

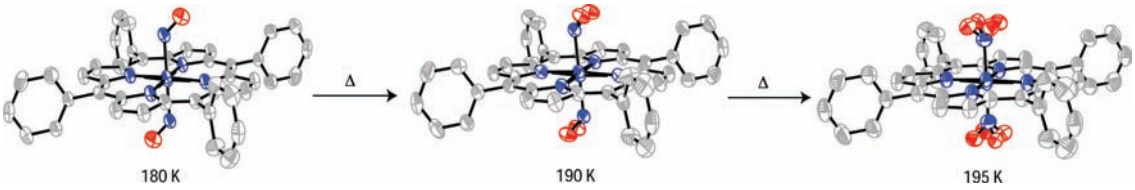

Figure 6. Three distinct observed structures of [Co(TPP)(NO)] characterized by varying degrees of disorder of the nitrosyl ligand. The two structures on the left-hand side of the diagram are found in a similar triclinic phase at those temperatures and lower, whereas the right-hand structure is found in a tetragonal phase at that temperature and higher. Reproduced from ref 28.

an intermediate structure with two unequally populated NO sites is observed near the transition temperature. Interestingly, the dihedral angle between the two Co−N−O planes is approximately 90°, consistent with reorganization to a single NO site.

A total of five different six-coordinate nitrosyls and two five-coordinate nitrosyls have had their X-ray structures determined at two or more temperatures. In all cases, the systems show greater nitrosyl ordering at lower temperatures in what appear to be a rather facile process for NO motion in the solid state. In the following two sections, we outline some further conclusions and details that can be drawn from these experimental results.

Structural Implications: What Have We Learned? The number of six-coordinate nitrosyl structures now available allow an examination of the effect, if any, of the relative orientation of NO on the observed vibrational spectra. The conclusions are simple: there appears to be little or no effect on the vibrational properties. Thus, an attempt to use the vibrational properties to define the rotational position of NO will not yield useful information. Temperature-dependent IR measurements[21] of the two crystalline polymorphs of [Fe(T*p*FPP)(1-MeIm)(NO)] over the temperature range of 106−350 K do provide further evidence that ν_{NO} is a good predictor of the trans Fe−N_{Im} bond distance changes in six-coordinate nitrosyl complexes. The value of ν_{NO} is not an absolute predictor of the trans distance because there are also effects of the porphyrin ligand (cis effects)[30] on the absolute value of the vibration. The total change in ν_{NO} can be as large as ∼30 cm^{-1} in six-coordinate nitrosyl derivatives with differing axial nitrogen ligands and trans distances.[16,18]

The observation that the multiple orientations of the NO ligand in room temperature structures of six-coordinate Fe(Porph)(1-MeIm)(NO)] derivatives could be frozen out at lower temperatures (∼100 K) was interesting. It strongly suggests that the NO orientations in these species are controlled by features qualitatively described as "crystal packing effects". The triclinic form of [Fe(T*p*FPP)(1-MeIm)(NO)] provided the most detailed and informative example of the five systems studied.[20,21] As shown earlier in Figure 3, this system was studied at a large number of temperatures between 100 and 350 K. Both the reversibility and the sensible temperature-dependent population of the two NO sites suggest that the experimental X-ray structural results define a solid-state equilibrium process. We analyzed[20] this system with the assumption that all crystallographic measurements of site populations represent thermal equilibrium positions:

$$\text{NO major orientation} \overset{K}{\rightleftharpoons} \text{NO minor orientation}$$

The thermodynamic parameters $\Delta H°$ and $\Delta S°$ of the system are then readily obtained from the van't Hoff relationship. Values obtained were $\Delta H° = 8.9 \pm 0.5$ kJ/mol and $\Delta S° = 17.2 \pm 1.4$ J/(mol K). The resulting small value of $\Delta G° = +3.8$ kJ/mol must reflect the differences in the free energies of the major and minor orientations caused by the intermolecular interactions. Similarly, small values of $\Delta G°$ were obtained from analysis of the temperature-dependent NO site populations in the monoclinic form of [Fe(T*p*FPP)(1-MeIm)(NO)] and [Fe(T*p*OCH_3PP)(1-MeIm)(NO)].

Analysis of the crystal packing effects examined nonbonded contacts between NO and the nearest atoms in its environment in tri-[Fe(T*p*FPP)(1-MeIm)(NO)]; representative NO orientations were evaluated [rotation around the Fe−N(NO) bond in increments of 10° while holding the remainder of the structure fixed].[20] The tabulation of the short van der Waals contacts reveals two regions that are favorable for the location of NO. The apparent relative merits of the two regions show temperature-dependent differences that are consistent with the observed NO population differences. This analysis shows that the temperature-dependent barrier to rotation decreases with increasing temperature. The two minima seen in this analysis are the result of bracketing of the NO ligand by peripheral *p*-fluorophenyl groups from different adjacent molecules. A more quantitative mapping can be done by calculating the potential energy as a function of NO orientation using the semiempirical nonbonded potential functions as originally outlined by Giglio[31] and expanded by Shmueli and Goldberg.[32] We have calculated the intermolecular interactions by the pairwise addition of all interactions involving the oxygen atom positions and all atoms in contact with the oxygen atoms at distances of less than the sum of the van der Waals radii. The results for the 100 and 350 K structures are displayed in Figure 7a. The energy difference between the two minima at 350 K is 6.2 kJ/mol.

The success of this analysis led us to analyze five additional six-coordinate examples.[20] The six different compounds involved a total of 23 independent structure determinations at temperatures ranging from 100 to 350 K. The results of the study are shown in Figure 7, which displays the calculated potential energies derived for the

(29) Patchkovskii, S.; Ziegler, T. *Inorg. Chem.* **2000**, *39*, 5354–5364.
(30) Buchler, J. W.; Kokisch, W.; Smith, P. D. *Struct. Bonding* (*Berlin*) **1978**, *34*, 79.
(31) Giglio, E. *Nature* **1969**, *222*, 339–341.
(32) Shmueli, U.; Goldberg, I. *Acta Crystallogr.* **1973**, *B29*, 2466–2471.

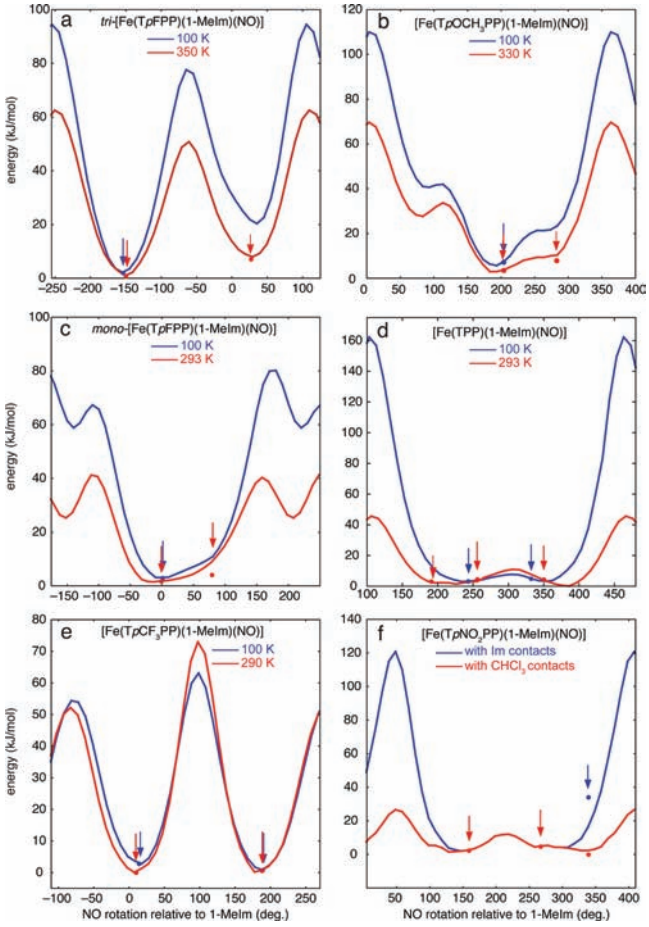

Figure 7. Potential energy diagrams for six [Fe(Porph)(NO)(1-MeIm)] complexes. Values are plotted for the lowest and highest temperatures for which structural data are available. The observed positions are shown as points and indicated by arrows. Reproduced from ref 20.

structures at the extremes of the temperatures measured. The observed NO motion (positions) ranges from movement between quite discrete positions to disorder best described by a continuum of positions over an angular range. However, in all cases, the analyses agree with the experimental observations. The TPP case (displayed in Figure 7d) shows the possible complexity of NO orientations. The broad valley of "acceptable" positions led in the original investigation to two observed orientations of NO[16] at room temperature to fit the experimental diffraction data, but three positions were required with higher resolution data.[20]

Theoretical Considerations. The results reported in the foregoing sections clearly suggest that the barriers to rotation around the Fe−N(NO) bond are quite small. Unfortunately, the experimental work provides only suggestive data about any orientation preferences. Should there be any preference for the relative orientation of the two axial ligands in a six-coordinate nitrosyl species, [Fe(Porph)(1-MeIm)(NO)]? Would the plane of the Fe−N−O group be parallel or perpendicular to the plane of the axial imidazole (Im) ligand? We utilized a series of DFT calculations to explore the relative energy differences for differing orientations of the NO and Im ligands with respect to the porphyrin core and an energy-minimized structure obtained for each position.[20] Figure 8 displays the calculated energies, with the lowest energy taken to be 0. In these calculations, the Im was held

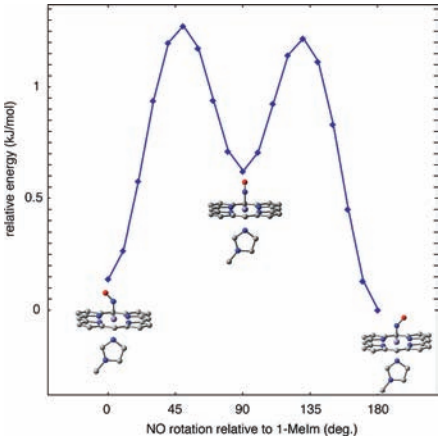

Figure 8. Potential energy landscape from DFT calculations exploring energy differences for varying relative orientations of the NO and Im ligands in [Fe(Porphine)(NO)(1-MeIm)]. The initial molecular configuration at 0° has the FeNO and 1-MeIm planes coplanar and pointing toward a *meso*-carbon atom. (Molecular energies were optimized at each FeNO orientation using the B3LYP functional with the VTZ basis set for iron and the 6-31G* basis set for all other atoms.) Reproduced from ref 20.

fixed with the plane along the line joining iron and the *meso*-carbon atom of the porphyrin core and with the NO rotated in 10° increments. The energy differences were less than 2 kJ/mol, but with the lowest energies occurring when the two axial ligand planes were parallel to each other. The perpendicular orientation showed a local minimum about 0.6 kJ/mol higher than the global minimum. The calculations are clearly in accordance with experimental observations in which the experimental structures tend toward the two axial ligands being nearly coplanar. As noted, the barriers to NO rotation are small (a barrier of less than 1.3 kJ/mol between the minima), with maxima occurring when the projections of NO are on the equatorial Fe−N_p bonds. These calculations are in agreement with the earlier theoretical study of Patchkovskii and Ziegler,[29] based on a coarser grid of NO rotations, that also suggested minimal rotational barriers and a global minimum when the two axial ligand planes are eclipsed. Our calculations also suggested a small increase in the Fe−N_{Im} bond length when the two ligands are 90° apart.

These calculations also provided insight into the structural effects of the orientation of the bound NO ligand and the induced asymmetry in the equatorial plane.[20] As noted earlier, this effect was first seen in several five-coordinate[23−25] iron nitrosyls and, subsequently, for six-coordinate species.[19,21] As shown by these new calculations, the rotation of the NO has effects on the equatorial bond distances, with the two equatorial bonds that bracket the projection of NO always shorter. The predicted difference of ∼0.015 Å is large enough to be experimentally significant. See Figure 9. An effect from rotation of the axial Im ligand is also predicted, but the difference is so small that it is unlikely to be observed experimentally. Although this asymmetry has been explored theoretically for the five-coordinate species,[33−35]

(33) Ghosh, A.; Wondimagegn, T. *J. Am. Chem. Soc.* **2000**, *122*, 8101.
(34) Leu, B. M.; Zgierski, M. Z.; Wyllie, G. R. A.; Scheidt, W. R.; Sturhahn, W.; Alp, E. E.; Durbin, S. M.; Sage, J. T. *J. Am. Chem. Soc.* **2004**, *126*, 4211–4227.
(35) Cheng, L.; Novozhilova, I.; Kim, C.; Kovalevsky, A.; Bagley, K. A.; Coppens, P.; Richter-Addo, G. B. *J. Am. Chem. Soc.* **2000**, *122*, 7142–7143.

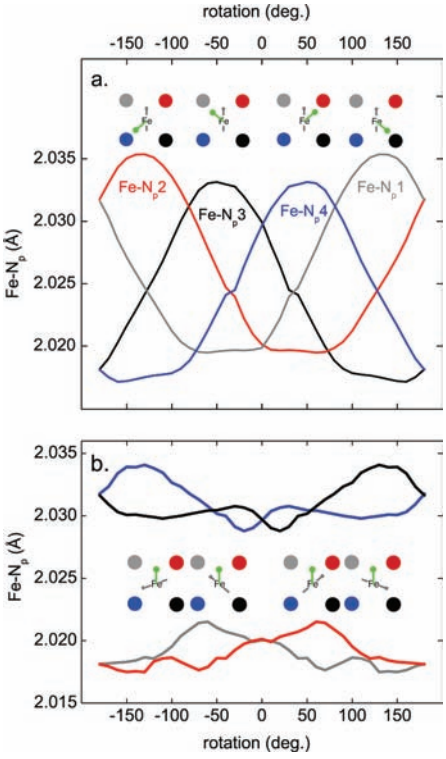

Figure 9. Variation in Fe−N_p bond lengths versus ligand orientation based on DFT calculations. The nitrogen atoms are labeled, clockwise starting from the upper left, as N_{p1} (gray), N_{p2} (red), N_{p3} (black), and N_{p4} (blue). At 0°, the FeNO and 1-MeIm planes are parallel, and the projection of the FeNO plane bisects Fe−N_{p1} and Fe−N_{p2} (looking down on the porphyrin plane with the NO ligand oriented toward the observer), whereas the 1-methyl group of the 1-MeIm plane also bisects Fe−N_{p1} and Fe−N_{p2}. In part a, the NO ligand is rotated with the Im orientation held fixed. In part b, the 1-MeIm ligand is rotated with the NO orientation held fixed. Reproduced from ref 20.

these calculations were the first to study the issue in six-coordinate complexes.

All of the structural studies described in the three sections above are clearly consistent with facile rotation of the NO ligand around the metal−ligand bond. The small barrier to rotation of the NO group around the Fe−N(NO) bond is calculated for both tetraaryl and porphine (no substituents) derivatives. It is likely that such small barriers are also applicable to naturally occurring hemes. Despite the relatively small energies involved between populating of the various sites, in the six-coordinate species, there is a tendency for the Fe−N−O and Im planes to be close to coplanar. The preference for this structural arrangement is supported by both the experimental and theoretical results.

Vibrational Dynamics of Iron in Nitrosyl Hemes

Vibrational spectroscopy is a highly sensitive probe of the heme structure. The C−O and Fe−CO stretching vibrations of heme−CO complexes, readily detected using conventional Raman[36] and IR[37] methods, strongly anticorrelate as a result of back-bonding from the Fe d_π orbitals into the CO π^* orbitals.[38,39] These frequencies are widely used to probe the local electric field, through the vibrational Stark effect, and the nature of the axial ligand trans to the CO.[39−44] Analogous frequencies are used to probe heme−NO and heme−O_2 complexes,[45−49] although the increased vibrational complexity of the nonlinear FeNO and FeO_2 fragments requires more care in structural interpretations of the observed vibrational frequencies.[50] Vibrations involving the other five bonds to the heme−Fe would provide equally valuable information on the heme structure but are less readily detectable using conventional spectroscopic methods.

NRVS reveals the complete vibrational density of states (VDOS) for an appropriately chosen Mössbauer isotope.[51,52] ^{57}Fe NRVS quantifies not only the frequencies but also the associated vibrational displacements of the iron.[53,54] Because the NRVS signal is proportional to the mean-square displacement of iron along the beam direction, measurements on oriented single crystals provide directional information as well.[55−58] Our measurements of iron vibrational dynamics in porphyrins have emphasized nitrosyl complexes,[34,54,56,57,59] but investigations of carbonyl complexes[58,60,61] provide a useful interpretational baseline.

(36) Kerr, E.; Yu, N.-T. Vibrational Modes of Coordinated CO, CN^-, O_2, and NO. *Biological Applications of Raman Spectroscopy*; Wiley-Interscience: New York, 1988; Vol. *3*, Chapter 2, pp 39−95.
(37) Dong, A.; Caughey, W. S. *Methods Enzymol.* **1994**, *232*, 139–175.
(38) Ray, G. B.; Li, X.-Y.; Ibers, J. A.; Sessler, J. L.; Spiro, T. G. *J. Am. Chem. Soc.* **1994**, *116*, 162–176.
(39) Spiro, T. G.; Wasbotten, I. H. *J. Inorg. Biochem.* **2005**, *99*, 34–44.
(40) Park, E. S.; Andrews, S. S.; Hu, R. B.; Boxer, S. G. *J. Phys. Chem. B* **1999**, *103*, 9813–9817.
(41) Phillips, G. N., Jr.; Teodoro, M. L.; Li, T. S.; Smith, B.; Olson, J. S. *J. Phys. Chem. B* **1999**, *103*, 8817–8829.
(42) Vogel, K. M.; Kozlowski, P. M.; Zgierski, M. Z.; Spiro, T. G. *Inorg. Chim. Acta* **2000**, *297*, 11–17.
(43) Park, E. S.; Boxer, S. G. *J. Phys. Chem. B* **2002**, *106*, 5800–5806.
(44) Franzen, S. *J. Am. Chem. Soc.* **2002**, *124*, 13271–13281.
(45) Potter, W. T.; Tucker, M. P.; Houtchens, R. A.; Caughey, W. S. *Biochemistry* **1987**, *26*, 4699–4707.
(46) Zhao, X.-J.; Sampath, V.; Caughey, W. S. *Biochem. Biophys. Res. Commun.* **1994**, *204*, 537–543.
(47) Benko, B.; Yu, N.-T. *Proc. Natl. Acad. Sci. U.S.A.* **1983**, *80*, 7042–7046.
(48) Tsubaki, M.; Yu, N.-T. *Proc. Natl. Acad. Sci. U.S.A.* **1981**, *78*, 3581–3585.
(49) Das, T.; Couture, M.; Ouellet, Y.; Guertin, M.; Rousseau, D. *Proc. Natl. Acad. Sci. U.S.A.* **2001**, *98*, 479–484.
(50) Vogel, K. M.; Kozlowski, P. M.; Zgierski, M. Z.; Spiro, T. G. *J. Am. Chem. Soc.* **1999**, *121*, 9915–9921.
(51) Sturhahn, W. *J. Phys.: Condens. Matter* **2004**, *16*, S497–S530.
(52) Zeng, W.; Silvernail, N. J.; Scheidt, W. R.; Sage, J. T. Nuclear Resonance Vibrational Spectroscopy (NRVS). In *Applications of Physical Methods to Inorganic and Bioinorganic Chemistry*; Scott, R. A., Lukehart, C. M., Eds.; Wiley: Chichester, U.K., 2007.
(53) Sage, J. T.; Durbin, S. M.; Sturhahn, W.; Wharton, D. C.; Champion, P. M.; Hession, P.; Sutter, J.; Alp, E. E. *Phys. Rev. Lett.* **2001**, *86*, 4966–4969.
(54) Sage, J. T.; Paxson, C.; Wyllie, G. R. A.; Sturhahn, W.; Durbin, S. M.; Champion, P. M.; Alp, E. E.; Scheidt, W. R. *J. Phys.: Condens. Matter* **2001**, *13*, 7707–7722.
(55) Rai, B. K.; Durbin, S. M.; Prohofsky, E. W.; Sage, J. T.; Ellison, M. K.; Scheidt, W. R.; Sturhahn, W.; Alp, E. E. *Phys. Rev. E* **2002**, *66*, 051904.
(56) Zeng, W.; Silvernail, N. J.; Wharton, D. C.; Georgiev, G. Y.; Leu, B. M.; Scheidt, W. R.; Zhao, J.; Sturhahn, W.; Alp, E. E.; Sage, J. T. *J. Am. Chem. Soc.* **2005**, *127*, 11200–11201.
(57) Silvernail, N. J.; Barabanschikov, A.; Pavlik, J. W.; Noll, B. C.; Zhao, J.; Alp, E. E.; Sturhahn, W.; Sage, J. T.; Scheidt, W. R. *J. Am. Chem. Soc.* **2007**, *129*, 2200–2201.
(58) Leu, B.; Silvernail, N.; Zgierski, M.; Wyllie, G.; Ellison, M.; Scheidt, W.; Zhao, J.; Sturhahn, W.; Alp, E.; Sage, J. *Biophys. J.* **2007**, *92*, 3764–3783.
(59) Rai, B. K.; Durbin, S. M.; Prohofsky, E. W.; Sage, J. T.; Wyllie, G. R. A.; Scheidt, W. R.; Sturhahn, W.; Alp, E. E. *Biophys. J.* **2002**, *82*, 2951–2963.
(60) Rai, B. K.; Durbin, S. M.; Prohofsky, E. W.; Sage, J. T.; Ellison, M. K.; Roth, A.; Scheidt, W. R.; Sturhahn, W.; Alp, E. E. *J. Am. Chem. Soc.* **2003**, *125*, 6927–6936.
(61) Leu, B. M.; Zgierski, M. Z.; Wyllie, G. R. A.; Ellison, M. K.; Scheidt, W. R.; Sturhahn, W.; Alp, E. E.; Durbin, S. M.; Sage, J. T. *J. Phys. Chem. Solids* **2005**, *99*, 2250–2256.

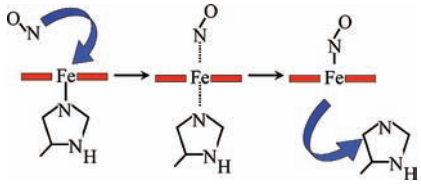

Figure 10. Diagram illustrating the trans-labilizing effect of the incoming NO ligand on the trans ligand.

Nitrosyl adducts of heme proteins present a richer vibrational profile than the superficially similar carbonyl adducts. This stems, in part, from the fact that NO binding weakens the bond to the trans ligand, which is the N_ε atom of a Im-His in many heme proteins, and in many cases ruptures this link to the protein, as schematically illustrated in Figure 10. As a result, five- and six-coordinate NO adducts of heme proteins are both commonly observed,[62−65] while five-coordinate CO complexes display a strong tendency to acquire a sixth ligand in aqueous solution and are therefore uncommon in proteins. Iron vibrational dynamics reflect the distinct electronic properties of five- and six-coordinate heme−NO complexes (see the following section). Here, we restrict our scope to nitrogen-bound ferrous heme nitrosyls and do not discuss the distinct vibrational properties of ferric nitrosyl hemes[66,67] or isonitrosyl isomers.[35]

The nonlinear FeNO unit is another factor that reduces the symmetry of the iron environment and enriches the vibrational dynamics of heme−NO complexes in comparison with the linear FeCO unit found in heme−CO complexes. Heme−CO complexes exhibit localized vibrations associated with stretching of the C−O and Fe−CO bonds and two degenerate modes associated with bending of the linear FeCO unit.[36,58] In contrast, the elastic energy required to distort the FeNO unit parallel or perpendicular to the FeNO plane differs as a consequence of its nonlinearity. Moreover, Fe−NO bending will alter the strength of the Fe−NO bond, implying that Fe−NO bending and Fe−NO stretching vibrations will interact significantly. In contrast, the nearly linear geometry of the FeCO unit[68−72] prevents mixing of the stretching and bending vibrations.

Figures 11 and 12 compare experimental and predicted VDOS for [Fe(TPP)(NO)] and [Fe(TPP)(1-MeIm)(NO)], respectively, which mimic the active site geometries of many five- and six-coordinate nitrosylated heme proteins. The experimental results (upper panel) include two distinct crystal orientations, characterizing iron motion along the directions parallel and perpendicular or nearly perpendicular to the

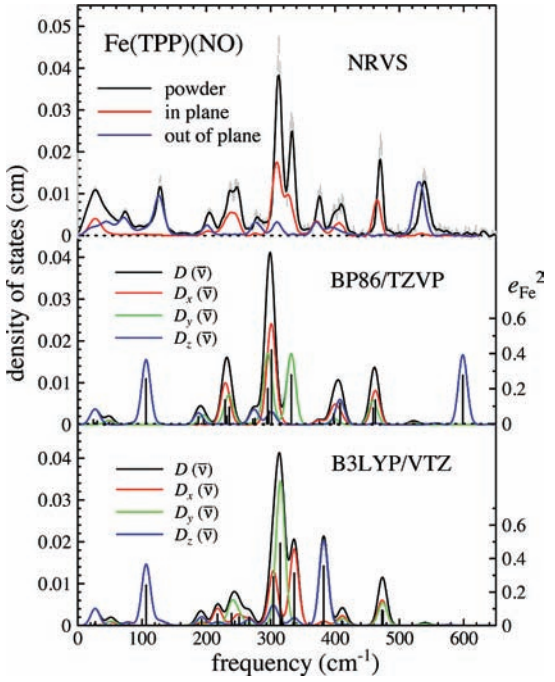

Figure 11. Quantum chemical predictions reproduce many features of the observed iron VDOS for [Fe(TPP)(NO)]. However, significant variations with the computational method include not only shifts larger than 200 cm^{-1} in the Fe−NO stretching frequency but also differences in the in-plane vibrational anisotropy, most noticeably near 340 cm^{-1}. In the upper panel, gray error bars represent the iron VDOS determined experimentally from NRVS measurements on a polycrystalline powder, while the black trace represents a five-point running average of these data, measured at 80 K. The red trace results from measurements on a single crystal oriented with the X-ray beam approximately parallel to all porphyrin planes, while the blue trace reflects a measurement with the X-ray beam parallel to the *c* axis of the tetragonal crystals, approximately the normal to all porphyrin planes. (Small variations result from the crystallographic phase change noted earlier;[22] the maximum possible error is 9°.) In-plane and out-of-plane crystal measurements were performed at 104 and 111 K, respectively. In the lower two panels, red, green, and blue traces represent predicted contributions from iron motion along the *x*, *y*, and *z* directions of a right-handed coordinate system, with the *z* axis orthogonal to the mean plane of the four pyrrole nitrogen atoms of the porphyrin and the *x* axis connecting the two methine carbon atoms lying closest to the FeNO plane. Computational methods are described in footnotes to Table 2.

mean plane of the porphyrin, and thus augment previously reported measurements on these compounds that compared a single crystal orientation with powder results.[34,56] Isotope substitution measurements supplement the experimental picture, yielding information on the vibrational dynamics of the ligand atoms.[56,73]

Calculations predict VDOS contributions from iron motion along all three directions, as shown in the lower panels. As discussed in the following section, the electronic structure, and consequently the vibrational predictions, varies significantly with the computational method. Nevertheless, both calculations shown in these figures correspond sufficiently well with observations to support a qualitative description of atomic motions associated with observed vibrational features. A comparison of the NRVS measurements on oriented single crystals with quantum chemical predictions yields a more comprehensive vibrational picture than that available from Raman measurements.

(62) Duprat, A. F.; Traylor, T. G.; Wu, G. Z.; Coletta, M.; Sharma, V. S.; Walda, K. N.; Magde, D. *Biochemistry* **1995**, *34*, 2634–2644.
(63) Deinum, G.; Stone, J. R.; Babcock, G. T.; Marletta, M. A. *Biochemistry* **1996**, *35*, 1540–1547.
(64) Lawson, D.; Stevenson, C.; Andrew, C.; Eady, R. *EMBO J.* **2000**, *19*, 5661–5671.
(65) Chan, N.-L.; Kavanaugh, J.; Rogers, P.; Arnone, A. *Biochemistry* **2004**, *43*, 118–132.
(66) Linder, D. P.; Rodgers, K. R. *Inorg. Chem.* **2005**, *44*, 1367–1380.
(67) Praneeth, V. K. K.; Paulat, F.; Berto, T. C.; George, S. D.; Nather, C.; Sulok, C. D.; Lehnert, N. *J. Am. Chem. Soc.* **2008**, *130*, 15288–15303.
(68) Ivanov, D.; Sage, J. T.; Keim, M.; Champion, P. M.; Powell, J. R.; Asher, S. A. *J. Am. Chem. Soc.* **1994**, *116*, 4139–4140.
(69) Lim, M.; Jackson, T. A.; Anfinrud, P. A. *Science* **1995**, *269*, 962–966.
(70) Sage, J. T.; Jee, W. *J. Mol. Biol.* **1997**, *274*, 21–26.
(71) Kachalova, G. S.; Popov, A. N.; Bartunik, H. D. *Science* **1999**, *284*, 473–476.
(72) Vojtěchovský, J.; Chu, K.; Berendzen, J.; Sweet, R.; Schlichting, I. *Biophys. J.* **1999**, *77*, 2153–2174.
(73) Paulat, F.; Berto, T.; George, S.; Goodrich, L.; Praneeth, V.; Sulok, C.; Lehnert, N. *Inorg. Chem.* **2008**, *47*, 11449–11451.

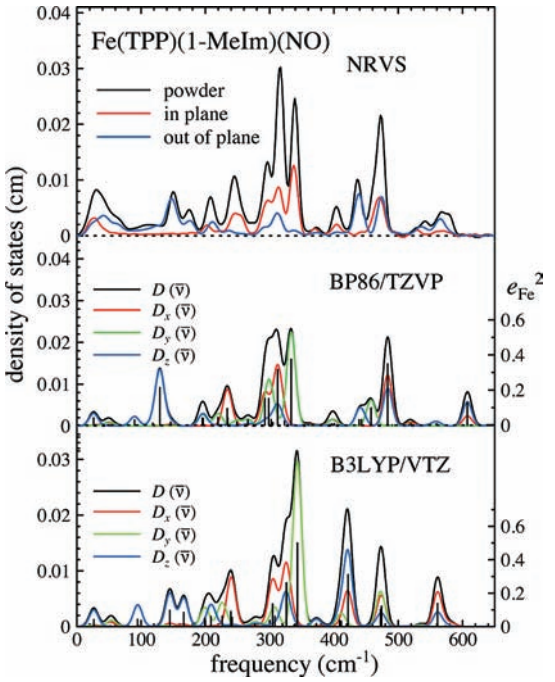

Figure 12. Calculations successfully reproduce most features of the iron VDOS observed for [Fe(TPP)(1-MeIm)(NO)]. Predicted contributions from Fe−NO stretching in the 400−500 cm^{-1} region are variable but less so than those for the five-coordinate complex (Figure 11). The color scheme and presentation for the experimental results (upper panel) and predictions (lower panels) are the same as those in Figure 12, except that the blue trace in the upper panel results from a measurement performed with the X-ray beam 13° from the plane of the pyrrole nitrogen atoms. In-plane and out-of-plane measurements were performed at 112 and 119 K, respectively, while the powder data indicate a sample temperature below 30 K. Computational methods are described in footnotes to Table 2.

FeNO Vibrations. Six-coordinate heme nitrosyls exhibit two vibrations associated with Fe−NO stretching and Fe−NO bending. Experimental characterization of the kinetic energy distribution (KED) of a mode near 560 cm^{-1} in MbNO reveals that it is highly localized on the FeNO unit, with most of the energy associated with motion of the nitrogen.[56] These data quantitatively support the mode character predicted for [Fe(TPP)(1-MeIm)(NO)], which is dominated by nitrogen motion in the FeNO plane along a direction nearly perpendicular to the N−O bond, visually resembling a pure Fe−NO bending motion. In spite of relatively weak enhancement in a spectrally congested region, this mode is readily identified in resonance Raman data because of the large isotope shift upon substitution of ^{15}NO for ^{14}NO.[56,74,75] Spiro and others have investigated this frequency as a probe of distal pocket interactions,[76] in analogy with the well-established sensitivity of the Fe−CO and C−O stretching frequencies to the local electric field.[39−44]

The experimental KED of a mode near 440 cm^{-1} exhibits less localization on the FeNO unit for MbNO but a larger iron displacement than the 560 cm^{-1} mode. NRVS measurements on oriented single crystals of the porphyrin model [Fe(TPP)(1-MeIm)(NO)] show that iron motion is nearly perpendicular to the porphyrin plane for a mode at 440 cm^{-1} (Figure 12).[56] Computational results on [Fe(TPP)(1-MeIm)(NO)] reveal a mode that exhibits stretching of the Fe−NO bond coupled with some NO rotation in the FeNO plane, as well as varying degrees of mixing with the ν_{50} porphyrin mode near 470 cm^{-1}, depending on the functional employed in the calculation. Although this mode is easily identified in the resonance Raman spectrum of MbNO,[47,56] the enhancement is significantly weaker for NO adducts of many ferrous heme proteins.[77−80]

NRVS results on five-coordinate nitrosyl porphyrins reveal a single localized FeNO vibration in the 520−540 cm^{-1} region. In contrast with the six-coordinate nitrosyl hemes, this mode is consistently strongly enhanced in resonance Raman measurements and has long been identified with stretching of the Fe−NO bond.[50,74,81] DFT calculations reproduce the pattern of iron amplitudes observed using NRVS and confirm the qualitative description as Fe−NO stretching, although, as with the six-coordinate heme−NO complexes, there is substantial mixing with Fe−NO bending. The mode character predicted for this mode resembles that predicted for the 440 cm^{-1} vibration of the six-coordinate complexes, and we associated the 70−100 cm^{-1} experimental frequency increase in the five-coordinate complexes with strengthening of the Fe−NO bond in the absence of the Im ligand.[56,73] Although the mode character predicted for the five-coordinate heme−NO complex is relatively independent of the computational method employed, it is notable that the predicted frequency varies by more than 200 cm^{-1} (see the following section)!

Analysis based on an empirical model for the molecular energy surface originally identified a mode at 470 cm^{-1} in [Fe(TPP)(NO)] with Fe−NO bending.[59] However, we observed no iron modes near this frequency in [Fe(OEP)(NO)], and DFT calculations predict that the 470 cm^{-1} frequency in [Fe(TPP)(NO)] corresponds to an in-plane porphyrin vibration (ν_{50}) with no significant Fe−NO bending contribution.[34] Although DFT calculations predict that Fe−NO bending contributes to a number of vibrations, we did not identify a single mode with primary Fe−NO bending character.[34]

Other Fe−Ligand Vibrations. Although vibrations of the remaining five Fe−ligand bonds are rarely identified in Raman spectra of six-coordinate hemes, all Fe−ligand vibrations contribute to the NRVS signal. Frequencies in the 300−350 cm^{-1} region dominate the VDOS reported for low-spin ferrous hemes (Figures 11 and 12),[54,56−59,34,60,61] while the strongest vibrational features of high-spin heme−Fe appear in the 210−260 cm^{-1} region.[53,55,82] These results

(74) Thomas, M. R.; Brown, D.; Franzen, S.; Boxer, S. G. *Biochemistry* **2001**, *40*, 15047–15056.
(75) Coyle, C. M.; Vogel, K. M.; Rush, T. S., I.; Kozlowski, P. M.; Williams, R.; Spiro, T. G.; Dou, Y.; Ikeda-Saito, M.; Olson, J. S.; Zgierski, M. Z. *Biochemistry* **2003**, *42*, 4896–4903.
(76) Ibrahim, M.; Xu, C.; Spiro, T. G. *J. Am. Chem. Soc.* **2006**, *51*, 16834–16845.
(77) Lukat-Rodgers, G. S.; Rodgers, K. R. *Biochemistry* **1997**, *36*, 4178–4187.
(78) Das, T. K.; Wilson, E. K.; Cutruzzola, F.; Brunori, M.; Rousseau, D. L. *Biochemistry* **2001**, *40*, 10774–10781.
(79) Sawai, H.; Makino, M.; Mizutani, Y.; Ohta, T.; Sugimoto, H.; Uno, T.; Kawada, N.; Yoshizato, K.; Kitagawa, T.; Shiro, Y. *Biochemistry* **2005**, *44*, 13257–13265.
(80) Andrew, C.; Kemper, L.; Busche, T.; Tiwari, A.; Kecskes, M.; Stafford, J.; Croft, L.; Lu, S.; Moenne-Loccoz, P.; Huston, W.; Moir, J.; Eady, R. *Biochemistry* **2005**, *44*, 8664–8672.
(81) Tomita, T.; Hirota, S.; Ogura, T.; Olson, J. S.; Kitagawa, T. *J. Phys. Chem. B* **1999**, *103*, 7044–7054.
(82) Budarz, T. E.; Prohofsky, E. W.; Durbin, S. M.; Sjodin, T. A.; Sage, J. T.; Sturhahn, W.; Alp, E. E. *J. Phys. Chem. B* **2003**, *107*, 11170–11177.

suggest a high sensitivity to the Fe spin state, and normal-mode analysis based either on empirical potential models or on DFT calculations associates these features with in-plane porphyrin vibrations (primarily ν_{53} and ν_{50} in the nomenclature introduced by Abe et al.[83]) that involve stretching of the Fe−N bonds to the pyrrole nitrogen atoms.[34,55,57−60,82]

For nitrosyl hemes, Fe−NO bending removes the nominal 4-fold symmetry of the iron environment and vibrational interactions will lift the degeneracy of the in-plane vibrations of the Fe−N_p bonds. In fact, predicted contributions to the in-plane VDOS differ significantly for iron motion parallel and perpendicular to the FeNO plane (Figures 11 and 12). However, ruffling and saddling distortions of the porphyrin, observed in crystal structures and sometimes in calculations, also reduce the nominal 4-fold symmetry. In six-coordinate porphyrins, the Im ligand lowers the symmetry of the iron environment as well. For example, we reported measurable iron vibrational anisotropy in the equatorial plane of six-coordinate carbonyl porphyrins, in spite of the linear FeCO unit.[58] NRVS measurements on single crystals of five-coordinate nitrosyl porphyrins with X-rays oriented along various in-plane directions will facilitate evaluation of the predicted alignment of the vibrational anisotropy with the FeNO plane.[84]

NRVS measurements recorded on oriented single crystals identify additional out-of-plane iron vibrations.[55−58] Calculations associate motion of the axial Im ligand with some of these. Fe-His vibrations are strongly enhanced in Raman scattering from five-coordinate ferrous hemes, excited in resonance with the heme Soret band, and have been widely used to probe the proximal environment in proteins.[85,86] A comparison of NRVS measurements with predictions identifies several vibrations involving Fe−Im motion in six-coordinate heme complexes, where Raman enhancement is weak.[57,58,60]

The capability to observe these vibrations in six-coordinate heme proteins using NRVS will provide many useful opportunities. For example, it would be useful to probe the extent to which hydrogen bonding modulates the character of the axial ligand in six-coordinate heme species on the peroxidase reaction cycle, expanding previous Raman characterizations of the Fe-His vibration in the nonphysiological five-coordinate ferrous species.[87,88] For nitrosyl hemes, these modes will probe the proposed weakening of the Fe−Im bond relative to carbonyl hemes. Fe−Im vibrations, as well as in-plane modes, respond sensitively to small changes in the Fe−N_{Im} bond length observed when [Fe(T*p*FPP)(1-MeIm)(NO)] crystallizes in different space groups.[57]

Molecular Distortion and Reactivity. In addition to Fe−ligand modes, NRVS provides a unique opportunity to identify low-frequency modes associated with molecular distortion. Modes below 200 cm^{-1} can be thermally activated and contribute to molecular reactivity. A particularly celebrated example is heme doming upon binding of a diatomic ligand. Heme doming has long been hypothesized to control cooperative oxygen binding in hemoglobin,[89,90] and identification of the associated frequencies will enable quantitative evaluation of the contribution of this motion to the free energy of cooperativity.

NRVS measurements on oriented single crystals provide direct evidence for iron vibrational motion orthogonal to the heme plane. Although Fe−Im vibrations may also contribute to vibrational motions in this region, low-frequency iron motion orthogonal to the heme plane is observed even for the five-coordinate complex Fe(TPP)(NO), where the Im ligand is absent. Modes at 73 and 128 cm^{-1} were previously reported.[34] Here, a comparison of the VDOS contributions due to iron motion parallel and perpendicular to the heme plane (Figure 11) identifies an additional out-of-plane mode at 44 cm^{-1} that is obscured by a broad feature attributable to acoustic lattice modes in the polycrystalline powder sample. Lattice modes form the primary contribution to the in-plane VDOS below 100 cm^{-1}, although a comparison with the out-of-plane VDOS indicates a weak in-plane vibration at 27 cm^{-1}.

For [Fe(TPP)(NO)], the dominant feature of the predicted out-of-plane iron VDOS at 106 cm^{-1} is clearly associated with heme doming, which is thus likely to contribute to one or more of the observed modes. The discrepancy between predicted and observed frequencies in this region may reflect computational limitations. For example, calculations on the isolated molecule take no account of intermolecular interactions that are likely to occur in the crystalline phase.

The out-of-plane VDOS observed for the six-coordinate complex [Fe(TPP)(1-MeIm)(NO)] below 200 cm^{-1} is somewhat more complex than that observed for [Fe(TPP)(NO)]. Calculations capture the increased complexity and indicate that Fe−Im vibrations as well as doming contribute to this frequency region. Further investigations of the low-frequency region will explore how factors including peripheral substituents on the porphyrin affect these frequencies and, we believe, allow quantitative estimates of the contribution of these motions to the free energy of ligand binding.

Vibrations as Probes of Molecular Geometry and Electronic Structure

One of the values of vibrational spectroscopy is the exquisite sensitivity of vibrational frequencies to the nuclear and electronic structure of molecules.[45−47,75,76] In particular, the frequencies of vibrations localized on an individual chemical bond usually correlate very strongly with the bond length[91−93] and can, in principle, be calibrated against known molecular structures.

(83) Abe, M.; Kitagawa, T.; Kyogoku, Y. *J. Chem. Phys.* **1978**, *69*, 4526–4534.
(84) Pavlik, J. W.; Barabanschikov, A.; Oliver, A. G.; Alp, E. E.; Sturhahn, W.; Zhao, J.; Sage, J. T.; Scheidt. W. R. *Angew. Chem., Int. Ed.* **2010**, in press DOI: 10.1002/anie.201000928.
(85) Kitagawa, T.; Nagai, K.; Tsubaki, M. *FEBS Lett.* **1979**, *104*, 376–378.
(86) Argade, P. V.; Sassaroli, M.; Rousseau, D. L.; Inubushi, T.; Ikeda-Saito, M.; Lapidot, A. *J. Am. Chem. Soc.* **1984**, *106*, 6593–6596.
(87) Teraoka, J.; Kitagawa, T. *J. Biol. Chem.* **1981**, *256*, 3969–3977.
(88) Smulevich, G.; Feis, A.; Howes, B. *Acc. Chem. Res.* **2005**, *38*, 433–440.
(89) Perutz, M. F. *Nature* **1970**, *228*, 726–734.
(90) Perutz, M. F.; Wilkinson, A. J.; Paoli, M.; Dodson, G. G. *Annu. Rev. Biophys. Biomol. Struct.* **1998**, *27*, 1–34.
(91) Badger, R. *J. Chem. Phys.* **1935**, *3*, 710–714.
(92) Green, M. T. *J. Am. Chem. Soc.* **2006**, *128*, 1902–1906.
(93) Dyer, R. B.; Woodruff, W. H. Vibrational Spectroscopy. In *Applications of Physical Methods to Inorganic and Bioinorganic Chemistry*; Scott, R. A., Lukehart, C. M., Eds.; Wiley: Chichester, U.K., 2007.

Heme−CO complexes exemplify the utility of vibrational spectroscopy as a probe of the molecular environment. Strong axial iron ligands trans to CO weaken the σ bond between iron and CO and decrease the Fe−CO frequency. On the other hand, variations in the degree of back-bonding from the Fe d_π orbitals into the empty CO π^* orbitals result in strongly anticorrelated changes in the Fe−C and C−O stretching frequencies.[38,39] Fe−C and C−O frequency variations have been calibrated against the local electric field and are widely exploited to probe proximal and distal heme environments in proteins.[39,41,43,44]

Heme nitrosyl vibrations also respond to the molecular environment. Although mixing of the Fe−NO stretching and Fe−NO bending character potentially complicates interpretation, the recent reassignment of the primary Fe−N stretching character in six-coordinate heme−NO complexes[56,73] indicates that the Fe−N frequency decreases by ~70 cm^{-1} upon binding of an axial Im ligand trans to NO. This observation is consistent with a 3 pm increase observed for the Fe−NO bond length in six-coordinate complexes.[19] A reduced N−O frequency for the six-coordinate complex, indicating a parallel increase in the N−O bond length, has long been established.[94]

The traditional description of the Fe−NO σ bond as resulting from interaction between the Fe d_{z^2} orbital and the NO π^* orbital parallel to the FeNO plane qualitatively rationalizes the observed influence of the trans axial ligand on the Fe−NO bonding.[95−97] The second axial ligand raises the energy of the Fe d_{z^2} orbital, reducing its mixing with the NO π^* orbital and weakening the Fe−N σ bond. The resulting increased population of the NO π^* orbital also accounts for the reduced N−O frequency in the six-coordinate complex. Electron paramagnetic resonance parameters, including hyperfine coupling with the nitrogen nucleus and orientation of the **g** tensor, are also consistent with an increased NO spin density in the six-coordinate complex.[97,98] These changes are paralleled by a decrease in the free energy for NO dissociation.[97,99]

Quantum Chemical Predictions. DFT generally predicts structures that compare well with crystallographic observations (Table 2). In addition to bond lengths and the Fe−N−O angle, optimized structures reproduce subtler details such as a small off-axis tilt of the Fe−N bond toward the oxygen atom and asymmetry in the Fe−N_p bonds to the heme, which are slightly shorter beneath the position of the oxygen atom.[24,33] Binding of a trans ligand increases the predicted spin density on the NO and decreases that on the iron, in qualitative agreement with the orbital argument.

When examined more quantitatively, predicted descriptions of the molecular geometry and electronic structure of heme−NO complexes vary considerably.[29,100,101] Ghosh has discussed the strong dependence of the predicted spin distribution on the functionals for several iron nitrosyl compounds, including nitrosyl hemes.[102,103] For both five- and six-coordinate heme−NO complexes, greater spin density appears on the NO for calculations performed with hybrid functionals such as B3LYP, which includes some exact exchange, than for pure functionals such as BP86.[102−104]

[Fe(TPP)(NO)] represents a particularly extreme case. We had previously noted that the B3LYP calculation exhibited "spin contamination".[34] We have repeated the calculation and observe that the predicted spin density has the opposite sign between iron and the nitrosyl, with the latter carrying nearly a full electronic spin. Although the Weiss model for heme−O_2 complexes attributes the singlet ground state to antiferromagnetic coupling between spin densities on iron and O_2, previous calculations predict little, if any, minority spin density for heme−NO complexes.[104] However, antiferromagnetic coupling of iron and NO spins is known for $S = {}^3/_2$ ground states of some nonheme iron nitrosyls.[103] Perhaps more interesting, computational models for the reduction of NO to N_2O at the heme/nonheme two-iron site of NO reductase predict spin densities of differing sign between the heme Fe and heme-bound NO.[105,106] It is conceivable that the appearance of a minority nitrosyl spin in the B3LYP calculation on [Fe(TPP)(NO)] may reflect a genuine electronic instability that protein active sites can exploit to modulate the reactivity of the heme−NO complex rather than merely a distracting computational anomaly.

In fact, there is no evidence that the B3LYP calculation correctly describes the electronic structure of [Fe(TPP)(NO)]. Predicted properties differing from those observed include an anomalously low Fe−NO frequency and a long Fe−N(NO) bond (Table 2). In contrast, no minority spin density results from the BP86 calculation, and less than 10% of the total spin density resides on NO. However, the vibrational predictions now diverge from observations in the opposite direction, with a Fe−NO frequency and bond length that are significantly higher and lower, respectively, than the observed values. One must conclude that neither calculation fully captures the electronic structure of [Fe(TPP)(NO)], although both reproduce other aspects of the observed VDOS well enough to support interpretation of the individual vibrational features.[34]

Axial vibrational motion due to Fe−NO stretching is also predicted at a lower frequency for B3LYP than for BP86 predictions in the six-coordinate [Fe(TPP)(1-MeIm)(NO)] complex (Figure 12), partially obscured by vibrational mixing of the Fe−NO stretching modes with the porphyrin vibration at 470 cm^{-1}. In each case, the experimental frequencies are intermediate between those predicted by B3LYP and BP86. These results

(94) Maxwell, J. C.; Caughey, W. S. *Biochemistry* **1976**, *15*, 388–396.
(95) Hoffmann, R.; Chen, M.-L.; Thorn, D. *Inorg. Chem.* **1977**, *16*, 503–511.
(96) Tangen, E.; Svadberg, A.; Ghosh, A. *Inorg. Chem.* **2005**, *44*, 7802–7805.
(97) Praneeth, V. K. K.; Näther, C.; Peters, G.; Lehnert, N. *Inorg. Chem.* **2006**, *45*, 2795–2811.
(98) Praneeth, V.; Neese, F.; Lehnert, N. *Inorg. Chem.* **2005**, *44*, 2570–2572.
(99) Traylor, T. G.; Sharma, V. S. *Biochemistry* **1992**, *31*, 2847–50.
(100) Rovira, C.; Kunc, K.; Hutter, J.; Ballone, P.; Parrinello, M. *J. Phys. Chem. A* **1997**, *101*, 8914–8925.
(101) Zhang, Y.; Gossman, W.; Oldfield, E. *J. Am. Chem. Soc.* **2003**, *125*, 16387–16396.
(102) Ghosh, A. *J. Biol. Inorg. Chem.* **2006**, *11*, 712–724.
(103) Hopmann, K.; Conradie, J.; Ghosh, A. *J. Phys. Chem. B* **2009**, *113*, 10540–10547.
(104) Radoń, M.; Pierloot, K. *J. Phys. Chem. A* **2008**, *112*, 11824–11832.
(105) Ohta, T.; Kitagawa, T.; Varotsis, C. *Inorg. Chem.* **2006**, *45*, 3187–3190.
(106) Blomberg, L.; Blomberg, M.; Siegbahn, P. *Biochim. Biophys. Acta* **2006**, *1757*, 240–252.

Table 2. Comparison of Experimental and Calculated Results[a]

			bond length (pm)		angle (deg)		frequency (cm^{-1})	
compound	method	integrated spin density on NO	Fe−NO	N−O	FeNO	FeN tilt	Fe−NO	N−O
Fe(TPP)(NO)	observation		173.9	116.3	144.4	6.3	539	1700
Fe(TPP)(NO)	B3LYP/VTZ[b]	−0.96	181.1	118.1	137.9	5.0	382.4	1775.3
Fe(TPP)(NO)	BP86/TZVP[c]	0.07	170.6	118.1	145.1	5.8	598.6	1691.7
Fe(TPP)(l-MeIm)(NO)	observation		175.0	118.2	137.7	1.8	440	1628
Fe(TPP)(l-MeIm)(NO)	B3LYP/VTZ[b]	0.81	178.0	117.5	139.4	2.2	421.9	1818.7
Fe(TPP)(l-MeIm)(NO)	BP86/TZVP[c]	0.40	174.2	118.6	140.0	3.3	483.5	1659.7

[a] DFT calculations used Gaussian 03 to optimize molecular geometry and determine vibrational frequencies and amplitudes. [b] Calculations with the B3LYP functional used the VTZ basis for Fe and 6-31G* for the remaining atoms. [c] Calculations with the BP86 functional used the TZVP basis for all atoms.

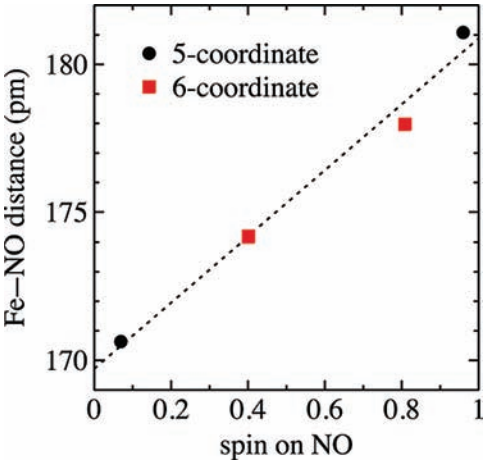

Figure 13. Significant variations in the predicted spin density on the NO ligand correlate with the predicted Fe−NO bond length. The four points include results calculated for Fe(TPP)(NO) and Fe(TPP)(1-MeIm)(NO), using both pure (BP86) and hybrid (B3LYP) functionals. The dashed line represents a least-squares fit.

appear to correlate with predicted variations in the reactivity, with hybrid functionals such as B3LYP consistently predicting lower NO dissociation energies than pure functionals such as BP86.[104,107]

The spin density predicted for both five- and six-coordinate heme−NO complexes consistently shows features resembling the NO π^* orbital in the FeNO plane and an Fe orbital with mixed d_{z^2}/d_{xz} character.[96,97] This suggests a description where variations in the contributions of these two orbitals to the Fe−NO σ-bonding orbital dominate variations in the electronic structure. We note that the net spin density on NO correlates with the predicted Fe−NO bond length when we include calculations on *both* five- and six-coordinate models (Figure 13).

Experimental Calibration of Quantum Chemical Predictions. Comparison of detailed information on iron vibrational dynamics with quantum chemical predictions is a two-way street. On one hand, the calculations presented here reproduce observed vibrational features with sufficient accuracy to support reliable descriptions of the corresponding normal modes. Such mode assignments will undoubtedly have value in interpreting vibrational data as probes of the molecular environment.

On the other hand, there are notable discrepancies between observed and predicted vibrational properties that depend on the computational method used. As a result, NRVS data provide a precise, quantitative experimental calibration that can be used to evaluate the success of electronic structure predictions, particularly for challenging cases such as the heme−NO complexes. The comprehensive, quantitative information on the frequency, amplitude, and direction of iron motion, derived experimentally from NRVS, renders it more valuable for this purpose than traditional vibrational spectroscopies.

In addition to variations in the predicted Fe−NO frequency described above, several other vibrational properties deviate significantly between the calculations described here. Neither B3LYP nor BP86 predictions reproduce all features of the experimental VDOS, and these calculations may, in fact, bracket the actual electronic structure.

Although both B3LYP and BP86 calculations superficially reproduce the splitting of the equatorial vibrations observed in the 300−340 cm^{-1} region of the orientationally averaged iron VDOS for [Fe(TPP)(NO)], significant differences appear upon examination of the directional contributions in Figure 11. In particular, the mode predicted near 340 cm^{-1} in the B3LYP calculation involves iron motion parallel to the FeNO plane, while iron motion is orthogonal to the FeNO plane for the analogous mode in the BP86 calculation. More specifically, the 337 cm^{-1} frequency predicted by B3LYP involves a large component of Fe−NO bending in the FeNO plane. In contrast, Fe−NO bending contributes most apparently to the 408 cm^{-1} mode in the BP86 calculation. Although the 332 cm^{-1} mode predicted by the BP86 calculation also involves significant displacement of iron and nitrogen atoms, this motion is now directed *perpendicular* to the FeNO plane. Unfortunately, we are unable to distinguish these possibilities experimentally for Fe(TPP)(NO), where crystallographic properties detailed above complicate the selection of a unique direction within the porphyrin plane. Measurements on compounds with a more favorable crystal structure may provide a more definitive test of these predicted differences in equatorial vibrational anisotropy.[84]

For the six-coordinate complex [Fe(TPP)(1-MeIm)(NO)], predicted contributions from vibration of the $Fe-N_{Im}$ bond to the Im also vary significantly with the method. The BP86 calculation predicts the largest iron amplitude below 200 cm^{-1} for the $Fe-N_{Im}$ stretching frequency at 129 cm^{-1}, while the B3LYP calculation predicts significant $Fe-N_{Im}$ character at higher frequency for two modes at 145 and 166 cm^{-1}, mixed with rotation of the Im in its own plane. The increased

(107) Oláh, J.; Harvey, J. *J. Phys. Chem. A* **2009**, *113*, 7338–7345.

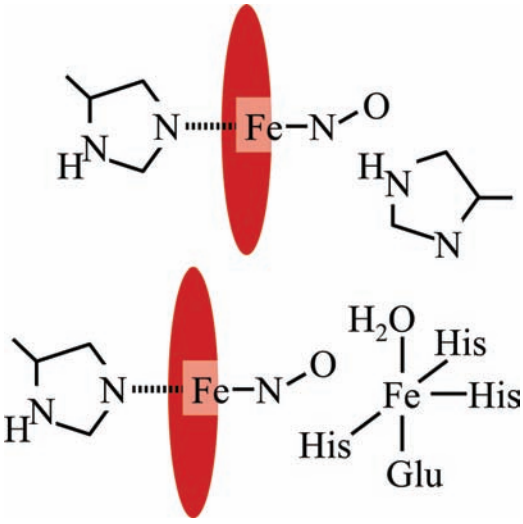

Figure 14. Proteins influence the electronic structure, vibrational dynamics, and biological activity of heme nitrosyls. (top) Polar amino acids influence observed vibrational properties of the FeNO unit. As an example, the distal histidine in myoglobin is within hydrogen-bonding distance of both nitrogen and oxygen atoms,[110] and mutation of this residue affects FeNO vibrational frequencies.[75] (bottom) Respiratory HCOs and NORs are phylogenetically related but exhibit distinct NO reactivity correlated with the identity of a nonheme metal adjacent to the heme. NO reversibly inhibits mammalian HCOs, which have copper in the nonheme site.[108] In contrast, NORs have iron in the nonheme site and reduce two molecules of NO to N_2O and water.[109] No X-ray structure has been reported for NOR, and the figure shows the coordination of the nonheme iron observed for the Fe_BMb enzyme designed to model the structure and reactivity of NOR.[111].

frequency for modes with Fe−N_{Im} character and the decreased frequency for modes with Fe−NO character predicted by the hybrid functional are consistent with the expected anticorrelation between the strengths of these two bonds.

Concluding Remarks

Knowledge of the electronic structure and dynamics of heme nitrosyls will form the basis for understanding how the molecular environment tunes their reactivity and determines their biological activity (Figure 14). At the simplest level, nonbonded interactions with surrounding groups restrict torsional freedom about the Fe−NO bond relative to the isolated molecule, entropically destabilizing the bound state. Electrostatic interactions are also likely to influence the heme−NO complex. In fact, vibrational properties of the FeNO unit vary in response to residue substitutions in myoglobin,[75] although hydrogen bonding with polar amino acids may not influence binding of NO as strongly as binding of O_2. A second nonheme metal is found near the heme in the catalytic sites of respiratory heme copper oxidases (HCOs) and bacterial nitric oxide reductases (NORs), and the identity and placement of the nonheme metal (Cu or Fe, respectively) is likely to determine NO's role as an inhibitor (in HCO) or as a substrate (in NOR).[108,109]

Quantum chemical calculations and spectroscopic observations will contribute synergistically to addressing such issues. A comparison of DFT calculations on both [Fe(TPP)(NO)] and [Fe(TPP)(1-MeIm)(NO)] indicates that vibrations of all Fe−ligand bonds are sensitive to predicted variations in the electronic structure. The calculations reproduce many structural features, guide the identification of observed vibrational features,[34,56,57] and provide a quantitative basis for understanding the torsional dynamics of the FeNO unit.[20] However, neither the B3LYP nor the BP86 functional succeeds in reproducing all observed features. A detailed comparison suggests that the primary difficulty lies with the correct description of the axial Fe−NO and Fe−N_{Im} bonding, although variations in the equatorial bonding are also noticeable.

Thus, a comparison of experimental and computational results suggests that a detailed experimental input such as that provided by NRVS may guide the theoretical development needed for a reliable description of the electronic structure. One possibility is that predictions of pure and hybrid functionals bracket the true electronic structure. In this case, intelligent interpolation between pure and hybrid predictions, guided by experimental observations, may lead to improved predictions of the electronic structure and reactivity. In general, heme−NO complexes appear to exhibit an unusual degree of variability with respect to the computational method, and one may be tempted to speculate that this variability hints at a genuine electronic instability that a protein can exploit to tune the reactivity.

Acknowledgment. We thank Dr. Marek Zgierski for early guidance in the structural optimization of porphyrins using DFT. We acknowledge financial support from the National Science Foundation (Grant PHY-0545787 to J.T.S.) and the National Institutes of Health (Grant GM-38401 to W.R.S.). Use of the Advanced Photon Source was supported by the U.S. Department of Energy, Basic Energy Sciences, Office of Science, under Contract DE-AC02-06CH11357.

(108) Brunori, M.; Forte, E.; Arese, M.; Mastronicola, D.; Giuffr, A.; Sarti, P. *Biochim. Biophys. Acta* **2006**, *1757*, 1144–1154.
(109) Moënne-Loccoz, P. *Nat. Prod. Rep.* **2007**, *24*, 610–620.
(110) Copeland, D. M.; West, A. H.; Richter-Addo, G. B. *Proteins: Struct., Funct., Genet.* **2003**, *53*, 182–192.
(111) Yeung, N.; Lin, Y.-W.; Gao, Y.-G.; Zhao, X.; Russell, B. S.; Lei, L.; Miner, K. D.; Robinson, H.; Lu, Y. *Nature* **2009**, *462*, 1079–1082.